

Capturing Carbon Dioxide from Air with Charged Sorbents

Huaiguang Li,^{ab} Mary E. Zick,^c Teedhat Trisukhon,^a Xinyu Liu,^a Helen Eastmond,^a Shivani Sharma,^a Tristan Spreng,^a Jack Taylor,^a Jamie W. Gittins,^a Cavan Farrow,^a Phillip J. Milner,^c Alexander C. Forse^{a*}

^aYusuf Hamied Department of Chemistry, University of Cambridge, Cambridge, CB2 1EW, United Kingdom

^bSchool of Science and Engineering, The Chinese University of Hong Kong, Shenzhen, Guangdong, 518172, China

^cDepartment of Chemistry and Chemical Biology, Cornell University, Ithaca, NY, 14850, United States

*corresponding author: acf50@cam.ac.uk

There is an urgent need for improved sorbents for the capture of carbon dioxide from the atmosphere, a process known as direct air capture. In particular, low-cost materials that can be regenerated at low temperatures would overcome the limitations of current technologies. In this work, we introduce an electrochemical method for preparing designer “charged-sorbent” materials and synthesise a hydroxide-functionalised activated carbon that can rapidly capture carbon dioxide from ambient air via (bi)carbonate formation. Unlike traditional bulk carbonates, material regeneration can be achieved at low temperatures (100 °C), and the sorbent's conductive nature permits direct Joule heating regeneration. Given their highly tailorable pore environments and low cost, we anticipate that charged-sorbents will find numerous potential applications in chemical separations, catalysis, and beyond.

1 **Introduction**

2 We face a global climate crisis. Emissions reduction and greenhouse gas removal from the
3 atmosphere are both necessary to achieve net-zero emissions and limit climate change.¹ A promising
4 approach towards negative emission technologies is direct air capture (DAC), whereby a sorbent
5 material selectively binds carbon dioxide from ambient air. The material is typically regenerated by
6 heating and/or applying reduced pressure, enabling carbon dioxide to be collected for geologic
7 storage or conversion. Existing DAC processes require large amounts of energy for material
8 regeneration. Thus, there is an urgent need to explore new energy-efficient approaches. For example,
9 rapid heating strategies that employ Joule heating (also known as resistive heating) have very recently
10 been explored and may reduce the costs associated with DAC.^{2,3}

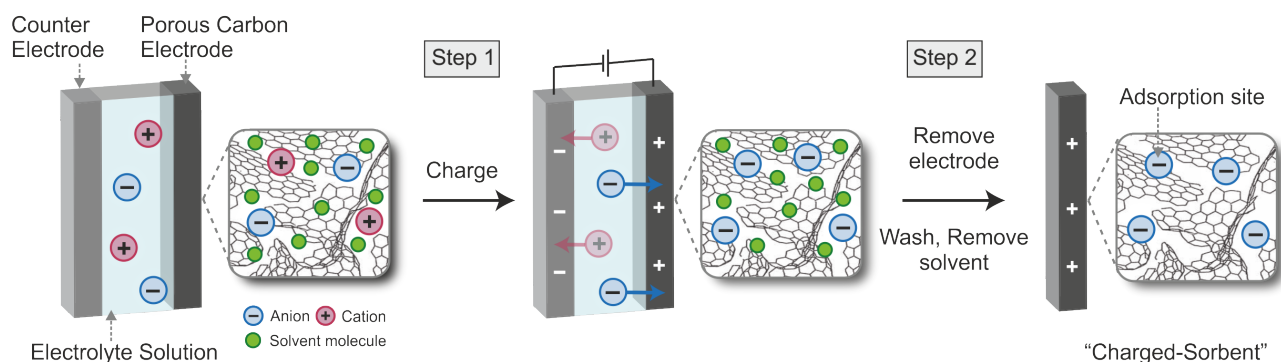
11 Hydroxide-based scrubbers are among the most promising for DAC.^{4,5} For example, an industrially
12 mature approach employs aqueous KOH solutions as the sorbent,⁶ but a high energy regeneration
13 step at 900 °C and the use of natural gas is required. A related approach under commercialisation uses
14 solid calcium hydroxide as the sorbent, again with regeneration at 900 °C.⁷ The high regeneration
15 temperatures arise from the significant lattice energy of the formed carbonate materials and contribute
16 greatly to the costs of running a DAC process. An alternative approach that can significantly reduce
17 regeneration temperatures is to disperse hydroxides in a porous material or polymer matrix.^{8,9} For
18 example, hydroxide-functionalised metal-organic frameworks have achieved promising performance
19 for DAC with much lower regeneration temperatures (~100 °C), but these materials suffer from
20 limited stabilities and high sorbent costs.¹⁰⁻¹²

21 Motivated by these challenges, we sought a low-cost and robust hydroxide material that could
22 combine DAC with low-temperature regeneration. We hypothesised that new DAC sorbents could
23 be synthesised by electrochemically inserting reactive hydroxide ions into a porous carbon
24 electrode.¹³⁻¹⁶ Here we achieve this concept, and show that hydroxide-based “charged-sorbents” can
25 capture CO₂ from ambient air, with the installed hydroxide sites reacting with CO₂ to form
26 (bi)carbonates. The materials have low regeneration temperatures and can be regenerated directly by
27 Joule heating without a secondary conductive support. Our electrochemical synthesis opens the door
28 to a wide palette of tuneable materials with applications ranging from separations to catalysis.

1 Results and Discussion

2 Preparation and characterisation of charged-sorbents

3 The preparation of charged-sorbents is based on the charging of an electrochemical energy storage
4 device (**Scheme 1**). During charging, electrolyte ions accumulate in the pores of a conductive porous
5 carbon electrode; for example, anions accumulate in the electrode when charging positively (**Scheme**
6 **1, step 1**). After completing the charging process, this electrode is removed from the cell and is
7 washed and dried to remove residual electrolyte and solvent to yield a charged-sorbent material. Our
8 hypothesis is that the accumulated ions in the porous electrode can then serve as active sites for an
9 adsorption process such as CO₂ capture. Different electrode materials, electrolyte ions, and solvents
10 can be selected, allowing for the preparation of tailored sorbents for different applications.

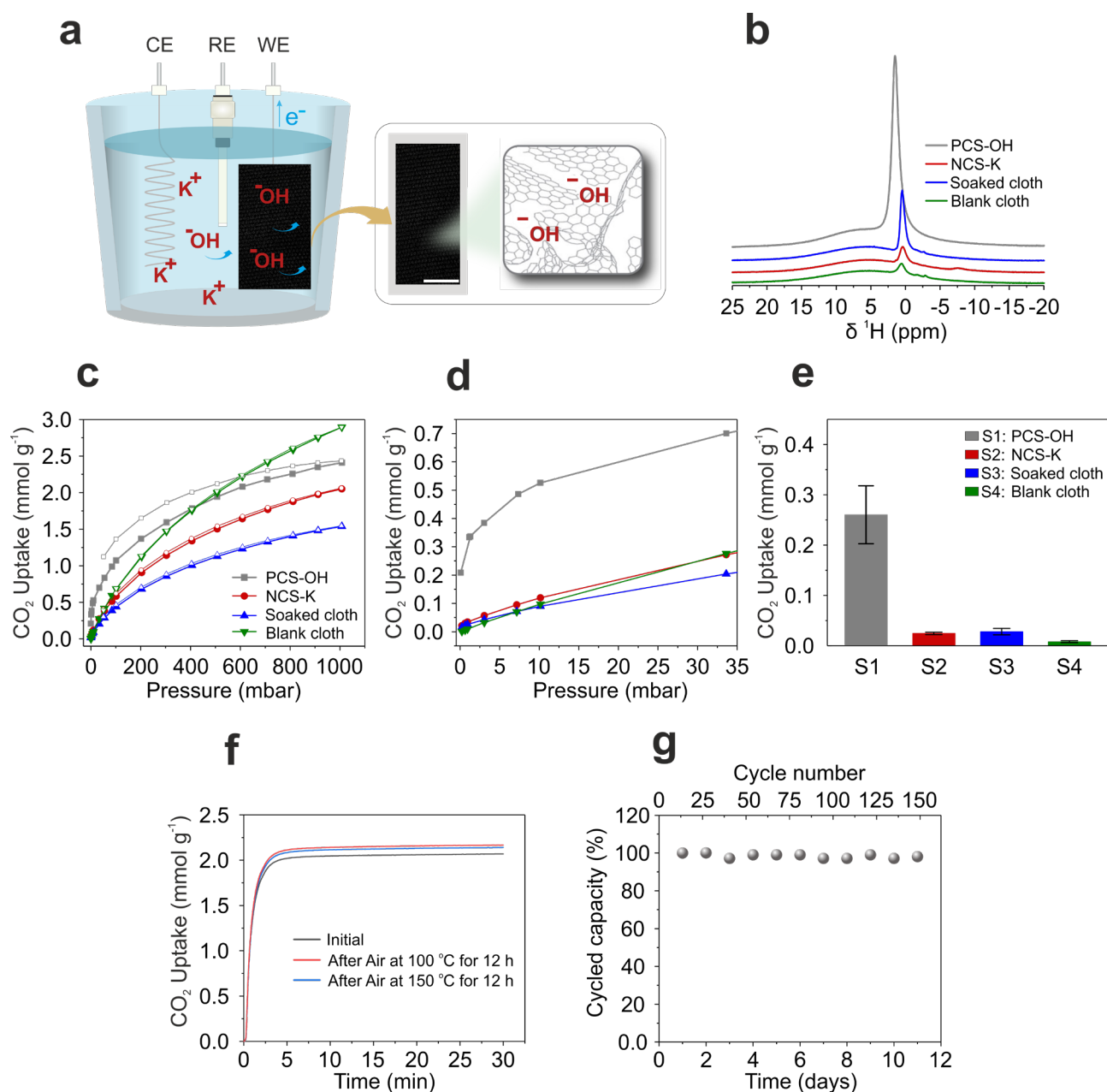


12 **Scheme 1:** Preparation of charged-sorbents: the porous carbon electrode is charged in an electrochemical cell (step 1).
13 The electrodes are removed from the cell, washed with deionised water, and evacuated to remove solvent molecules
14 (shown as green circles) to yield charged-sorbents (step 2). The activated carbon schematic is adapted from Ref.¹⁷.

15 Using this approach, we targeted a hydroxide-functionalised porous carbon as a new sorbent for DAC.
16 This was achieved by using inexpensive activated carbon cloth as the electrode (**Fig. S1**) and a 6 M
17 KOH (aq.) solution (**Fig. 1a**). The activated carbon cloth was positively charged by applying a
18 potential of +0.565 V vs. SHE for 4 hours, thereby accumulating reactive hydroxide ions within the
19 carbon pores. Both capacitive and faradaic currents were observed during charging, suggesting that
20 hydroxides are accumulated through both electric double-layer formation and oxidation of surface
21 functional groups (**Fig. S2, Table S1**). Following charging, the electrode was removed from the cell,
22 and was washed and dried to yield the final positively charged-sorbent (PCS) bearing hydroxide ions,
23 referred to as **PCS-OH (Fig. 1a)**. Powder X-ray diffraction analysis showed no reflections from
24 crystalline KOH or related products, suggesting that the hydroxide ions are incorporated primarily
25 within the nano-meter sized pores of **PCS-OH (Fig. S3)**. Finally, the counterpart negatively charged-
26 sorbent was prepared as a control sample by applying a potential of -0.235 V vs. SHE for 4 hours, to
27 yield a negatively charged-sorbent replete with potassium ions (NCS-K).

1 Evidence for the incorporation of hydroxide ions in the pores of **PCS-OH** was obtained from ^1H
2 solid-state NMR measurements (**Fig. 1b**). For **PCS-OH**, a strong resonance was observed at ~ 1.5
3 ppm, corresponding to OH^- species present in the pores. This assignment was supported by control
4 measurements on the as-purchased activated carbon cloth (“blank cloth”), a carbon cloth that was
5 soaked in the electrolyte but not charged, (“soaked cloth”), and the negatively charged carbon cloth
6 sample NCS-K, which all revealed much weaker ^1H resonances assigned to small amounts of residual
7 H_2O or OH^- species. The more positive ^1H chemical shift in **PCS-OH** likely arises from differences
8 in the ring current effects from the charged aromatic carbon surfaces.^{18,19} Combustion analysis also
9 supports an increased amount of hydrogen in **PCS-OH** compared to the controls (**Fig. S4**), further
10 supporting the charge-driven accumulation of OH^- species in the electrode.

11 Gas sorption experiments further support the accumulation of hydroxide ions in the pores of **PCS-**
12 **OH** (**Fig. S5**). The Brunauer-Emmett-Teller surface area of **PCS-OH** was $920 \text{ m}^2 \text{ g}^{-1}$, 20% lower
13 than the blank cloth ($1175 \text{ m}^2 \text{ g}^{-1}$) (**Fig. S5**). We hypothesise that the 20% reduction in surface area
14 for **PCS-OH** compared to the blank cloth arises due to two factors: (i) the accumulation of hydroxide
15 ions in the pores reducing the accessible pore volume, and (ii) the electrochemical oxidation of
16 functional groups in the carbon (**Fig. S2 and Table S1, Section 2**) disrupting the carbon’s overall
17 porosity. Despite the small decrease in the material surface area, **PCS-OH** remains highly porous
18 (**Fig. S5c**), suggesting that the accumulated hydroxide ions should be accessible as reactive sites for
19 CO_2 adsorption.



1

2 **Fig. 1. Preparation of hydroxide charged-sorbent and CO₂ sorption.** **a)** Scheme of charging activated carbon fabric
 3 ACC-5092-10 cloth in 6 M KOH via a three-electrode configuration. Scale bar: 0.5 cm. **b)** ¹H solid-state NMR (9.4 T)
 4 spectra of PCS-OH and control samples, acquired at a MAS rate of 12.5 kHz. **c)** CO₂ adsorption (filled data points) and
 5 desorption (hollow data points) isotherms of PCS-OH and control samples at 25 °C. **d)** Low-pressure region of the CO₂
 6 adsorption isotherms from (c). **e)** CO₂ uptake of PCS-OH and control samples at 0.4 mbar and 25 °C. Standard deviations
 7 are calculated from 5 independent samples. **f)** Dry, pure CO₂ uptake curves at 40 °C and 1 bar CO₂ for PCS-OH after
 8 activation under flowing dry N₂ at 130 °C for 1 h (gray curve), after exposure to flowing dry air (~21% O₂ in N₂) at
 9 100 °C for 12 h (red curve), and after exposure to flowing dry air (~21% O₂ in N₂) at 150 °C for 12 h (blue curve). **g)**
 10 Cycling capacities for 150 adsorption/desorption cycles for the PCS-OH in a simulated temperature-pressure swing
 11 adsorption process (Fig. S9). Adsorption: 30 °C, 20 min; Desorption: 100 °C, 20 min; dry 30% CO₂ in N₂.

12 Excitingly, CO₂ adsorption isotherm measurements (**Fig 1c, d, e**) revealed enhanced CO₂ capture at
 13 low pressures for **PCS-OH** relative to the control samples. This enhanced low pressure uptake is
 14 typical of hydroxide-functionalised sorbents,^{10,11} supporting CO₂ chemisorption by the accumulated

1 hydroxide ions. Consistent with this finding, the adsorption enthalpy (ΔH_{ads}) of **PCS-OH** was
2 calculated to be $-52 \pm 24 \text{ kJ mol}^{-1}$ (**Fig. S5d, e**). Importantly, **PCS-OH** exhibited increased CO₂
3 uptake at CO₂ partial pressures relevant to DAC. At 0.4 mbar and 25 °C, the CO₂ capacity for **PCS-**
4 **OH** is $0.26 \pm 0.06 \text{ mmol g}^{-1}$ (10 independent samples, **Fig S6**), which is significantly larger than the
5 capacities of the control samples under these conditions (**Fig. 1d, e**). Finally, our charged-sorbents
6 are highly tuneable materials, since the electrode (and electrolyte) can readily be varied in the
7 synthesis. As a second example, powdered activated carbon was first prepared into a free-standing
8 electrode film before synthesising the charged-sorbent (Fig. S8, see Methods **Section 2**). Enhanced
9 low pressure CO₂ uptake was again observed, demonstrating the generality of the charged-sorbent
10 approach (**Fig. S8**).

11 In addition to the promising gas sorption results, thermogravimetric analysis (TGA) measurements
12 indicate that **PCS-OH** has promising thermal and oxidative stability. The sorbent was heated to
13 150 °C under flowing dry air at atmospheric pressure for 12 h. Dry, pure CO₂ adsorption isobars
14 before and after air exposure showed very similar capacities and uptake kinetics, confirming the
15 oxidative stability of the material under these conditions (**Fig. 1f**). This oxidative stability is in
16 contrast to the behaviour of amine-based sorbents, which typically display poor oxidative stability, a
17 recurring challenge for their application for DAC.^{20,21} A simulated temperature-pressure swing
18 adsorption process was carried out to interrogate cycling stability. **PCS-OH** was subjected to 150
19 adsorption and desorption cycles using TGA under concentrated CO₂ conditions (30% CO₂ in N₂)
20 (**Fig. 1g and Fig. S9**). Consistent with the thermal stability test, **PCS-OH** exhibited a stable cycling
21 capacity (assuming negligible N₂ uptake), with minimal performance loss after 150 cycles. Low
22 regeneration temperatures of 100 °C can be used (**Fig. S10**), supporting the idea that dispersal of the
23 reactive hydroxides in the carbon pore network prevents the formation of stable bulk carbonates.
24 Overall, these data support that **PCS-OH** exhibits remarkable stability and affinity towards CO₂ at
25 pressures relevant to DAC.

1 CO₂ Capture mechanism

2 To investigate the mechanistic pathway responsible for strong CO₂ binding in **PCS-OH**, we collected
3 ¹³C solid-state NMR (ssNMR) spectra for **PCS-OH** and the control samples after dosing with ¹³CO₂
4 gas (**Fig. 2a**). All samples revealed strong
5 resonances at 119 ppm and weaker resonances
6 at 125 ppm, which are assigned to physisorbed
7 CO₂ in the carbon nanopores and free ¹³CO₂
8 gas, respectively.²² The chemical shift
9 difference between these species is consistent
10 with a ring current shielding for the in-pore
11 physisorbed species, with the shift difference of
12 -6 ppm similar to a recent NMR study on other
13 carbon cloths.^{23,24} In contrast to the controls, the
14 spectrum of **PCS-OH** revealed an additional
15 resonance at 156.0 ppm, assigned to
16 chemisorbed (bi)carbonate species (**Fig. 2b**).²⁵⁻
17 ²⁸ This provides strong evidence that the
18 hydroxide sites incorporated through our
19 electrochemical synthesis chemically react with
20 CO₂. The chemical shift of 156.0 ppm is similar
21 to bulk potassium bicarbonate (161.4 ppm, **Fig.**
22 **S12**), with the smaller value in **PCS-OH** arising
23 from ring-current effects and supporting that the
24 (bi)carbonate species reside in the carbon
25 nanopores (**Fig. 2b**). Quantitative
26 measurements showed that the amount of
27 physisorbed CO₂ in the four sorbents is similar
28 (around 1 mmol g⁻¹), while only **PCS-OH**
29 chemisorbs CO₂ (0.95 mmol g⁻¹ at 0.94 bar)
30 (**Fig. 2c**). These results further allow us to
31 estimate a lower limit for the hydroxide content
32 in **PCS-OH** of 0.95 mmol g⁻¹, assuming a 1:1

33 reactivity of CO₂ and hydroxide, as well as an estimated molecular formula for **PCS-OH** of (OH)C₈₈.
34 Overall, these experiments strongly support that reactive ions can be installed in porous carbon
35 through our electrochemical synthesis to achieve greatly enhanced reversible CO₂ sorption.

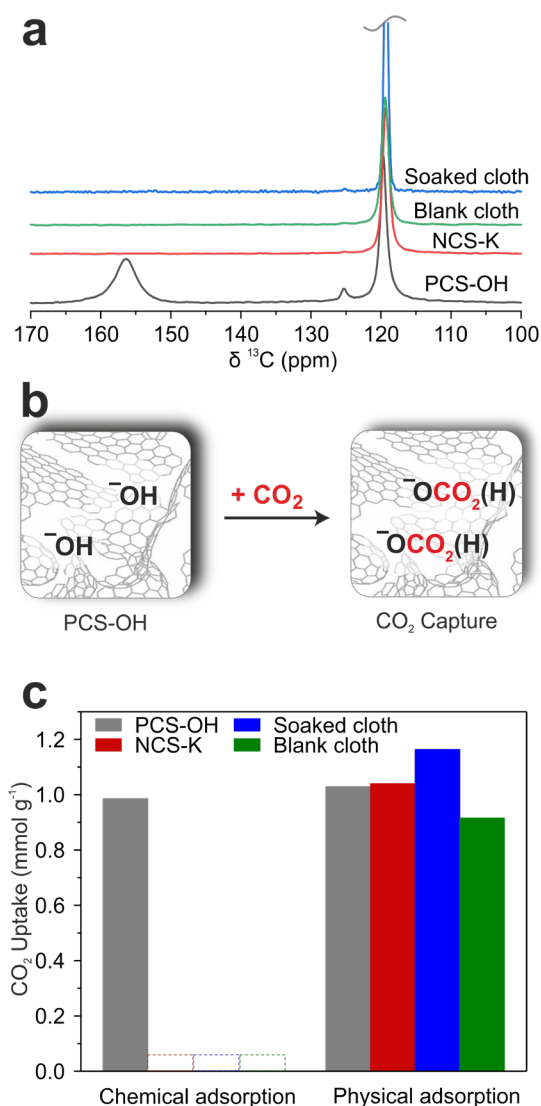
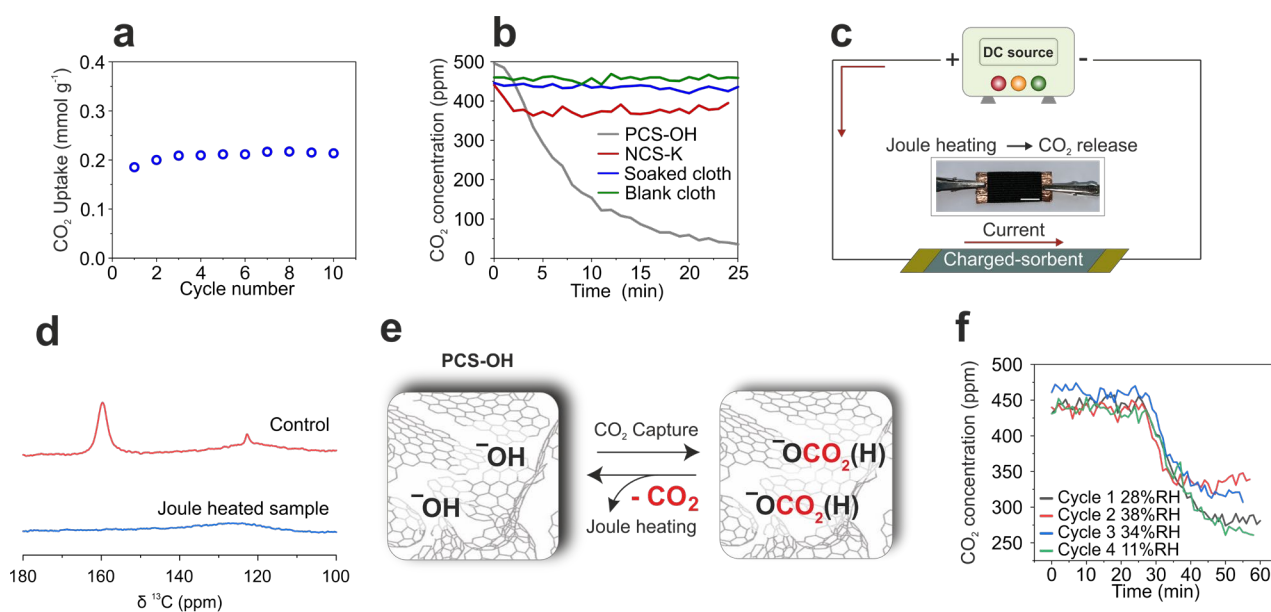


Fig. 2. Most probable CO₂ binding site proposed from ssNMR experiments. a) Quantitative ¹³C solid-state NMR spectra of sorbents with ¹³CO₂ gas dosing at the pressure of 0.9 bar, acquired at a MAS rate of 12.5 kHz (see Fig. S11 for a control experiment with no CO₂ dosing). b) Proposed mechanism for CO₂ capture by positively (hydroxide) charged-sorbent. c) CO₂ uptake of sorbents via chemical and physical adsorption calculated from resonances at 156 ppm and 119 ppm of (a), respectively.

1 Demonstration of DAC and regeneration by Joule heating

2 The promising low-pressure CO₂ uptake of **PCS-OH** through chemisorption motivated direct air
3 capture tests. DAC performance was initially evaluated under simulated dry air with 400 ppm CO₂
4 at 30 °C, with desorption conducted under 100% N₂ at 130 °C. These measurements revealed a CO₂
5 capacity of approximately 0.2 mmol g⁻¹, similar to the isotherm measurements, which was stable over
6 repeated adsorption and desorption cycles (**Fig 3a**). The DAC kinetics are promising, with a
7 calculated CO₂ capture rate of 7.5 mmol CO₂ g⁻¹ h⁻¹, which is around 7 times faster than for typical
8 amine-functionalized sorbents (**Fig. S13 and Table S2**).



9

10 **Fig. 3. DAC and Joule heating regeneration.** a) Cycling capacities of DAC for 10 adsorption/desorption cycles for
11 PCS-OH from TGA measurements. Adsorption: 30 °C, 60 min, 400 ppm CO₂ in dry air; Desorption: 130 °C, 60 min,
12 100% N₂. The cycled capacity (difference) is shown. b) DAC measurements in a sealed box filled with air at 37% RH.
13 The mass of PCS-OH is 120 mg. c) Schematic of Joule heating for CO₂ release (Scale bar: 0.5 cm). d) ¹³C ssNMR spectra
14 of sorbents with ¹³CO₂ gas dosing at 0.9 bar: after exposure to the air for 20 min without joule heating (control sample,
15 red curve); after 20 min Joule heating around 90 °C in air (blue curve). MAS rate of 12.5 kHz. e) Proposed mechanism
16 for CO₂ release from positively (hydroxide) charged-sorbent via Joule heating. f) DAC experiments for PCS-OH, with
17 Joule heating regeneration under nitrogen between cycles. The mass of PCS-OH in f) is 33 mg.

18 As a more realistic DAC test, freshly activated **PCS-OH** and the three control samples were subjected
19 to ambient air in a sealed container equipped with a CO₂ sensor. Excitingly, a large decrease in CO₂
20 concentration was observed for **PCS-OH**, with a decrease from 500 ppm to around 25 ppm (a 475
21 ppm decrease) in 25 min. In contrast, the CO₂ concentration decreased much less for the control
22 samples (**Fig 3b**). These measurements strongly support that our electrochemical synthesis enhances
23 carbon capture at low partial pressures and enables DAC.

1 The electrically conductive nature of our **PCS-OH** sorbent opens the door to regeneration by direct
2 Joule heating,²⁵ a strategy that leads to rapid regeneration times compared to traditional heating
3 methods.² In contrast to previous approaches that required the use of electrically conductive
4 supports,² here we directly attach electrodes to our conductive sorbent for Joule heating (**Fig 3c**). A
5 DC voltage of 7–8 V was applied across a piece of **PCS-OH** (2 cm x 1 cm), resulting in the rapid
6 heating of the material to ~90 °C within ~1 minute. Solid-state NMR experiments on samples pre-
7 dosed with ¹³CO₂ gas showed that Joule heating led to the complete release of adsorbed CO₂ species
8 in this time (**Fig. 3d, e**). We then carried out a proof-of-concept DAC cycles with ambient air (**Fig.**
9 **3e, f**) and dry air (**Fig. S14**), with regeneration by Joule heating in nitrogen. The regenerated **PCS-**
10 **OH** was then reused in the next DAC cycle, with a total of 5 cycles completed. The experiments
11 display reversible CO₂ capture over 5 cycles both in dry and humid conditions (**Fig. S14, Fig 3e, f**).
12 Our results show that our charged-sorbents can be regenerated by direct Joule heating without the
13 need for a secondary conductive support material.

14 We finally explored the role of relative humidity (RH) on the CO₂ capture performance of **PCS-OH**,
15 as water deteriorates the CO₂ capacity of many OH⁻ based materials.^{10,26} While **PCS-OH** could
16 capture CO₂ in humid air (**Fig. 3f**), we found that water co-adsorption is detrimental to the material's
17 CO₂ uptake. The effect of pre-adsorbed water (at ~53% RH at 25 °C) on the CO₂ capacity was
18 examined through quantitative ¹³C ssNMR (**Fig. S15**). The CO₂ adsorption capacity of **PCS-OH**
19 under humid conditions was half of that of under dry conditions, but chemisorption was still observed.
20 Promisingly, Joule heating regenerates the CO₂ capacity of the sorbent under humid conditions (**Fig.**
21 **3e and S13**). Therefore the reduction in CO₂ capacity is likely due to filling of the hydrophilic pores
22 with H₂O (**Fig. S16**), blocking access of CO₂ to reactive OH⁻ sites,¹⁰ rather than due to sorbent
23 degradation. Ultimately, further work must be done to understand the effects of water on these
24 materials and to optimise a full DAC process with Joule heating. With further optimisation and
25 scaling, we anticipate that Joule heating regeneration will lead to a rapid temperature-pressure swing
26 DAC process driven by renewable electricity.

1 Outlook

2 Charged-sorbents are a new low-cost materials class with highly tuneable chemical structures. Our
3 electrochemical synthesis method accumulates reactive ions in the sorbent pores, with these species
4 then serving as reactive sites in an adsorptive process. Targeting direct air capture (DAC) of carbon
5 dioxide as a representative separation, we achieved the electrochemical insertion of hydroxide ions
6 into activated carbon electrodes, with the resulting charged-sorbent material showing enhanced CO₂
7 uptake at low pressures due to chemisorption to form (bi)carbonates. The materials capture CO₂
8 directly from the air and can be regenerated at low temperatures of 90-100 °C. The electrical
9 conductivity of charged-sorbents enables material regeneration by direct Joule heating, with no need
10 for separate heating equipment. We hypothesise that with further optimisation, a rapid energy-
11 efficient DAC process can be achieved that requires renewable electricity as the only input. The low
12 cost of activated carbons and the electrolytes used here is promising from an applications standpoint.
13 Beyond DAC, we anticipate that the readily tuneable nature of our charged-sorbent materials, where
14 the electrolyte and electrode can easily be varied, will lead to a family of new materials with a wide
15 range of applications.

16 References

- 17 1. Board, O. S., National Academies of Sciences, & Medicine. Negative Emissions
18 Technologies and Reliable Sequestration: A Research Agenda. *National Academies Press*,
19 *Washington D.C* (2019).
- 20 2. Lee, W. H. *et al.* Sorbent-Coated Carbon Fibers for Direct Air Capture Using Electrically-
21 Driven Temperature Swing Adsorption. SSRN Scholarly Paper at
22 <https://doi.org/10.2139/ssrn.4274414> (2022).
- 23 3. Xia, D. *et al.* Electrically Heatable Graphene Aerogels as Nanoparticle Supports in
24 Adsorptive Desulfurization and High-Pressure CO₂ Capture. *Adv. Funct. Mater.* **30**, 2002788
25 (2020).
- 26 4. Forse, A. C. & Milner, P. J. New chemistry for enhanced carbon capture: beyond
27 ammonium carbamates. *Chem. Sci.* **12**, 508–516 (2021).
- 28 5. Zick, M. E., Cho, D., Ling, J. & Milner, P. J. Carbon Capture Beyond Amines: CO₂
29 Sorption at Nucleophilic Oxygen Sites in Materials. *ChemNanoMat* **n/a**, e202200436.
- 30 6. Keith, D. W., Holmes, G., St. Angelo, D. & Heidel, K. A Process for Capturing CO₂ from
31 the Atmosphere. *Joule* **2**, 1573–1594 (2018).
- 32 7. Noah, M., Ghoussoub, Mireille, Mills, Jennifer, & Scholten, Max. A scalable direct air
33 capture process based on accelerated weathering of calcium hydroxide. [https://uploads-
34 ssl.webflow.com/6041330ff151737fb03fc474/6245ecce7b2d1b514b674816_Heirloom%20White%
35 20Paper.pdf](https://uploads-ssl.webflow.com/6041330ff151737fb03fc474/6245ecce7b2d1b514b674816_Heirloom%20White%20Paper.pdf) (2018).
- 36 8. Wang, T., Lackner, K. S. & Wright, A. Moisture Swing Sorbent for Carbon Dioxide
37 Capture from Ambient Air. *Environ. Sci. Technol.* **45**, 6670–6675 (2011).

- 1 9. Shi, X. *et al.* Sorbents for the Direct Capture of CO₂ from Ambient Air. *Angew. Chem. Int.*
2 *Ed.* **59**, 6984–7006 (2020).
- 3 10. Bien, C. E. *et al.* Bioinspired Metal–Organic Framework for Trace CO₂ Capture. *J. Am.*
4 *Chem. Soc.* **140**, 12662–12666 (2018).
- 5 11. Liao, P.-Q. *et al.* Monodentate Hydroxide as a Super Strong Yet Reversible Active Site for
6 CO₂ Capture from High-humidity Flue Gas. *Energy Environ. Sci.* **8**, 1011–1016 (2015).
- 7 12. Wright, A. M. *et al.* A Structural Mimic of Carbonic Anhydrase in a Metal–Organic
8 Framework. *Chem* **4**, 2894–2901 (2018).
- 9 13. Shi, X. *et al.* Moisture-Driven CO₂ Sorbents. *Joule* **4**, 1823–1837 (2020).
- 10 14. Shi, X., Xiao, H., Lackner, K. S. & Chen, X. Capture CO₂ from Ambient Air Using
11 Nanoconfined Ion Hydration. *Angew. Chem. Int. Ed.* **55**, 4026–4029 (2016).
- 12 15. Forse, A. C., Merlet, C., Griffin, J. M. & Grey, C. P. New Perspectives on the Charging
13 Mechanisms of Supercapacitors. *J. Am. Chem. Soc.* **138**, 5731–5744 (2016).
- 14 16. Salanne, M. *et al.* Efficient Storage Mechanisms for Building Better Supercapacitors. *Nat.*
15 *Energy* **1**, 1–10 (2016).
- 16 17. Harris, P. J. F. Fullerene-like models for microporous carbon. *J. Mater. Sci.* **48**, 565–577
17 (2013).
- 18 18. Forse, A. C., Griffin, J. M., Presser, V., Gogotsi, Y. & Grey, C. P. Ring Current Effects:
19 Factors Affecting the NMR Chemical Shift of Molecules Adsorbed on Porous Carbons. *J. Phys.*
20 *Chem. C* **118**, 7508–7514 (2014).
- 21 19. Anderson, R. J. *et al.* NMR Methods for Characterizing the Pore Structures and Hydrogen
22 Storage Properties of Microporous Carbons. *J. Am. Chem. Soc.* **132**, 8618–8626 (2010).
- 23 20. Gouedard, C., Picq, D., Launay, F. & Carrette, P.-L. Amine degradation in CO₂ capture. I. A
24 review. *Int. J. Greenh. Gas Control* **10**, 244–270 (2012).
- 25 21. Reynolds, A. J., Verheyen, T. V., Adeloju, S. B., Meuleman, E. & Feron, P. Towards
26 commercial scale postcombustion capture of CO₂ with monoethanolamine solvent: Key
27 considerations for solvent management and environmental impacts. *Environ. Sci. Technol.* **46**,
28 3643–3654 (2012).
- 29 22. Mafra, L. *et al.* Structure of Chemisorbed CO₂ Species in Amine-Functionalized
30 Mesoporous Silicas Studied by Solid-State NMR and Computer Modeling. *J. Am. Chem. Soc.* **139**,
31 389–408 (2017).
- 32 23. Forse, A. C., Merlet, C., Grey, C. P. & Griffin, J. M. NMR Studies of Adsorption and
33 Diffusion in Porous Carbonaceous Materials. *Prog. Nucl. Magn. Reson. Spectrosc.* **124–125**, 57–84
34 (2021).
- 35 24. Bi, S. *et al.* Permselective Ion Electrosorption of Subnanometer Pores at High Molar
36 Strength Enables Capacitive Deionization of Saline Water. *Sustain. Energy Fuels* **4**, 1285–1295
37 (2020).
- 38 25. Sadiq, M. M. *et al.* A Pilot-Scale Demonstration of Mobile Direct Air Capture Using Metal-
39 Organic Frameworks. *Adv. Sustain. Syst.* **4**, 2000101 (2020).

- 1 26. Zick, M. E., Pugh, S. M., Lee, J.-H., Forse, A. C. & Milner, P. J. Carbon Dioxide Capture at
2 Nucleophilic Hydroxide Sites in Oxidation-Resistant Cyclodextrin-Based Metal–Organic
3 Frameworks. *Angew. Chem. Int. Ed.* **61**, e202206718 (2022).
- 4 27. Greenspan, L. Humidity Fixed Points of Binary Saturated Aqueous Solutions. *J. Res. Natl.*
5 *Bur. Stand. Sect. Phys. Chem.* **81A**, 89–96 (1977).
- 6 28. Forse, A. C. *et al.* Elucidating CO₂ Chemisorption in Diamine-Appended Metal–Organic
7 Frameworks. *J. Am. Chem. Soc.* **140**, 18016–18031 (2018).
- 8 29. Forse, A. C. *et al.* NMR Study of Ion Dynamics and Charge Storage in Ionic Liquid
9 Supercapacitors. *J. Am. Chem. Soc.* **137**, 7231–7242 (2015).

1 **Methods**

2 **Section 1: Materials and Methods**

3 **Chemicals:** Activated carbon fabric ACC-5092-10 cloth was purchased from Kynol. The cloth was
4 activated for 1 h at 100 °C in a vacuum oven before use. Potassium hydroxide (99%), potassium
5 bicarbonate (99%), and sodium hydroxide (99%) were purchased from Sigma-Aldrich. All chemicals
6 were of analytical grade and directly used as received without further purification.

7 **Electrochemistry:** All electrochemical measurements were performed at room temperature using a
8 BioLogic SP-150 potentiostat and a Biologic BCS-800 Series. A coiled platinum wire (BASi, MW-
9 1033) was used as a counter electrode. In three electrode measurements, the reference electrode was
10 Hg/HgO (ALS, RE-61AP) with 0.1 M KOH filling solution; the filling solution was exchanged
11 routinely to keep the potential constant. Potentials are converted to the standard hydrogen electrode
12 (SHE) using the correction $E_{\text{SHE}} = E_{\text{Hg/HgO}} + 0.165 \text{ V}$.

13 **Elemental analysis:** C, H and N wt% were determined via CHN combustion analysis using an Exeter
14 Analytical CE-440, with combustion at 975 °C.

15 **Volumetric gas sorption measurements:** N₂ isotherms were collected using an Autosorb iQ gas
16 adsorption analyzer at 77 K. The BET surface area was determined by the BET equation and
17 Rouquerol's consistency criteria implemented in AsiQwin. All pore size distribution fittings were
18 conducted in AsiQwin using N₂ at 77 K on carbon (slit-shaped pores) quenched solid density
19 functional theory (QSDFT) model. CO₂ sorption isotherms were also collected on an Autosorb iQ
20 gas adsorption analyzer. Isotherms conducted at 25, 35, and 45 °C were measured using a circulating
21 water bath. Samples were activated at 100 °C in vacuum for 15 h prior to gas sorption measurements.

22 **Thermogravimetric gas sorption measurements:** Thermogravimetric CO₂ adsorption experiments
23 were conducted with a flow rate of 60 mL/min using a TA Instruments TGA Q5000 equipped with a
24 Blending Gas Delivery Module. Samples were activated under flowing N₂ for 30 min at various
25 temperatures prior to cooling to 30 °C and switching the gas stream to CO₂ mixtures. Cycling
26 experiments were carried out on a Mettler Toledo TGA / DSC 2 Star^{ed} system equipped with a Huber
27 mini chiller. The adsorption and desorption of CO₂ were performed at 30 °C and 100 °C for 20 min
28 under 30% CO₂ and 70% N₂ with a flow rate of 140 mL/min, respectively.

29 **X-ray diffraction (XRD):** Powder X-ray diffraction (PXRD) patterns were collected on a Malvern
30 Panalytical Empyrean instrument equipped with an X'celerator Scientific detector using a non-
31 monochromated Cu K α source ($\lambda = 1.5406 \text{ \AA}$). The data were collected at room temperature over a
32 2θ range of 3–80 °, with an effective step size of 0.017 °.

1 **Scanning electron microscopy (SEM):** Samples were mounted onto a stainless-steel SEM stub
2 using adhesive carbon tape. SEM imaging was performed on a Tescan MIRA3 FEG-SEM. Analysis
3 of SEM images was conducted using the FIJI ImageJ software.

4 **NMR spectroscopy:** Solid-state NMR experiments were performed with a Bruker Advance
5 spectrometer operating at a magnetic field strength of 9.4 T, corresponding to a ^1H Larmor frequency
6 of 400.1 MHz. A Bruker 4 mm HX double resonance probe was used in all cases. ^1H NMR spectra
7 were referenced relative to neat adamantane ($\text{C}_{10}\text{H}_{16}$) at 1.9 ppm and ^{13}C NMR spectra were
8 referenced relative to neat adamantane ($\text{C}_{10}\text{H}_{16}$) at 38.5 ppm (left-hand resonance). All of the NMR
9 tests were conducted with a sample magic angle spinning rate of 12.5 kHz. A 90° pulse-acquire
10 sequence was used in each experiment. For ^{13}C NMR experiments, recycle delays were set to be more
11 than five times the spin-lattice relaxation time for each sample to ensure that the experiments were
12 quantitative.

13 Charged-sorbents with different water contents were prepared for the NMR characterization. The
14 sorbents were kept in a closed container for 24 h under different relative humidities (RH). Saturated
15 KCl and $\text{Mg}(\text{NO}_3)_2$ solutions were used to maintain 53% RH at 25°C , respectively.²⁷

16 **$^{13}\text{CO}_2$ dosing for solid-state NMR experiments:** Freshly activated samples (75°C , vacuum oven,
17 24 h) were packed into 4 mm NMR rotors in air and then evacuated for a minimum of 10 min in a
18 home-built gas manifold.²⁸ ^{13}C -enriched CO_2 gas (Sigma Aldrich, <3 atom % ^{18}O , 99.0 atom % ^{13}C)
19 was then used to dose the samples with gas at room temperature until the gas pressure stabilised,
20 before the rotors were sealed inside the gas manifold with a mechanical plunger.

21 **DAC tests in sealed chambers:** The DAC tests were carried out in a sealed box (volume ~ 600 mL)
22 with a CO_2 sensor (Aranet4) to record the concentration of CO_2 , temperature and RH at every one-
23 minute interval. Before each cycle, the box was exposed to fresh air until the CO_2 concentration, RH
24 and temperature stabilized. The sorbent was then placed in the box, which was sealed during
25 measurements.

26 **Joule heating:** After each DAC adsorption step, the sorbent was extracted from the box and
27 connected with an external power source for Joule heating. A BioLogic SP-150 potentiostat was used
28 to vary the electrical input. A constant voltage was applied and adjusted during the experiment to
29 achieve a sample temperature in a range of 85 – 95°C under an N_2 atmosphere. The temperature was
30 monitored using a thermocouple at a single contact point. After Joule heating regeneration, the
31 electrode was reused for another DAC adsorption cycle.

32 **Section 2: Preparation of charged-sorbents**

1 Three-electrode method:

2 The charged-sorbents were prepared in a three-electrode configuration with a home-made cell, a
3 Hg/HgO (in 0.1 M KOH) reference electrode and a platinum wire counter electrode. The activated
4 carbon fabric ACC-5092-10 cloth (2 cm × 2 cm) was charged with a constant potential for 4 hours
5 (0.565 V vs SHE for the PCS-OH and -0.235 V vs SHE for NCS-K, respectively) in 40 mL of 6 M
6 KOH (aq.) via chronoamperometry (CA) (Fig S2). After completing the charging process, the charged
7 cloth was removed and held by plastic tweezers and rinsed with deionized water from a wash bottle
8 for 5 min in total on both sides. 500 mL deionized water in total was used to wash off the residual
9 KOH solution. The rinsed cloth was then placed in the vacuum oven at 75 °C for 24 h to remove the
10 remaining water.

11 For the “soaked” control sample, the activated carbon fabric ACC-5092-10 cloth (2 cm × 2 cm) was
12 soaked in 40 mL of 6 M KOH for 4 h. After soaking, the same rinsing and drying processes used for
13 the charged-sorbents was carried out.

14 Two-electrode Swagelok method:

15 Free-standing carbon films were prepared by adapting the published literature method.²⁹ In brief,
16 YP80F activated carbon powder (95 wt %) (Kuraray Chemical, Japan) was mixed with
17 polytetrafluoroethylene binder (5 wt %) (Sigma-Aldrich, 60 wt % dispersion in water) in ethanol.
18 The resulting slurry was kneaded and rolled to give a carbon film of approximately 0.25 mm thickness,
19 followed by removing residual solvent at 100 °C in vacuum for at least 24 h. Disk-shaped electrodes
20 were then cut from the carbon films using a 0.25 inch hole punch. Symmetrical Swagelok
21 electrochemical cells were then prepared in Swagelok PFA-820-6 fittings with stainless steel current
22 collectors, YP80F film electrodes (for both the positive and negative electrodes), 6 M KOH (aq.)
23 electrolyte, and a glass fibre separator (Whatman glass microfiber filter (GF/A)). Cells were charged
24 at a constant cell voltage of 0.8 V for 4 hours in two electrode mode, and the positive electrode was
25 then extracted, washed, and dried, as above, to yield a charged-sorbent referred to as PCS-OH
26 (YP80F). Three samples from three independent electrochemical cells were combined to provide
27 sufficient material for gas sorption measurements.

28 **Section 3: Heats of adsorption calculation**

29 CO₂ adsorption isotherms at different temperatures were fit using the Dual-Site Freundlich-Langmuir
30 model (Eq. S1), where $Q(P)$ is the predicted uptake CO₂ at pressure P in mmol g⁻¹, $Q_{sat,i}$ is the
31 saturation pressure of binding site i in mmol g⁻¹, b_i is the Langmuir parameter of site i , v_i is the

1 Freundlich parameter of site i . The isotherms were fit with v_1 and v_2 set as 1 (Dual-Site Langmuir
2 model). Fits were obtained using Origin software.

$$3 \quad Q(P) = \frac{Q_{sat1}(b_1P)^{v_1}}{1 + (b_1P)^{v_1}} + \frac{Q_{sat2}(b_2P)^{v_2}}{1 + (b_2P)^{v_2}}$$

4 Eq. S1

5 Heats of adsorption ($-\Delta H_{ads}$) were calculated using the Clausius-Clapeyron equation (Eq. S2), where
6 P_Q are pressure values corresponding to the same loading Q , ΔH_{ads} is the differential enthalpy of
7 adsorption in kJ mol^{-1} , R is the ideal gas constant, T is the temperature in K, and c is a constant. Fits
8 over a range of Q values were obtained using Mathematica to calculate the differential enthalpies of
9 adsorption (ΔH_{ads}) based on the slopes of the linear trendlines fit to $\ln(P_Q)$ vs $1/T$ at constant values
10 of Q .

$$11 \quad \ln(P_Q) = \left(\frac{\Delta H_{ads}}{R}\right)\left(\frac{1}{T}\right) + c$$

12 Eq. S2

13 **Acknowledgments**

14 This work was supported by an EPSRC New Horizons award (EP/V048090/1), a Leverhulme Trust
15 Research Project Grant (RPG-2020-337), and a UKRI Future Leaders Fellowship to A.C.F.
16 (MR/T043024/1). Further support was from the U.S. Department of Energy, Office of Science, Office
17 of Basic Energy Sciences under Award Number DE-SC0021000 and by a Research-to-Impact Fast
18 Grant awarded by the 2030 Project and the Cornell Atkinson Center for Sustainability (M.E.Z.,
19 P.J.M.).

20 **Competing interests**

21 H.L., H.E. and A.C.F. are authors of a submitted patent on charged-sorbents.

Supplementary Information for

Capturing Carbon Dioxide from Air with Charged-Sorbents

Huaiguang Li,^{ab} Mary E. Zick,^c Teedhat Trisukhon,^a Xinyu Liu,^a Helen Eastmond,^a Shivani Sharma,^a Tristan Spreng,^a Jack Taylor,^a Jamie W. Gittins,^a Cavan Farrow,^a Phillip J. Milner,^c Alexander C. Forse^{a*}

^aYusuf Hamied Department of Chemistry, University of Cambridge, Cambridge, CB2 1EW, United Kingdom

^bSchool of Science and Engineering, The Chinese University of Hong Kong, Shenzhen, Guangdong, 518172, China

^cDepartment of Chemistry and Chemical Biology, Cornell University, Ithaca, NY, 14850, United States

*corresponding author: acf50@cam.ac.uk

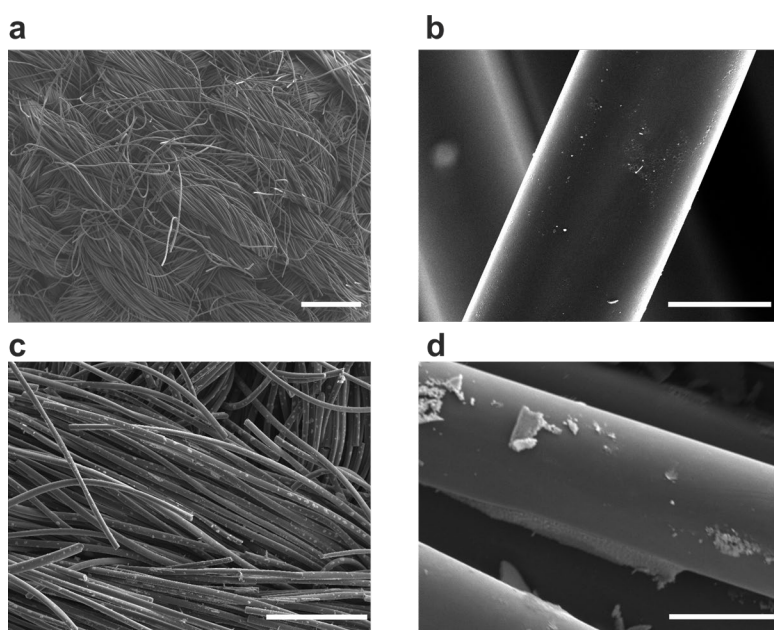


Fig. S1. Scanning electron microscopic images of activated carbon fabric ACC-5092-10 cloth before (a), (b) and after (c), (d) charging, with scale bars of (a) (c) 500 μm and (b) (d) 10 μm .

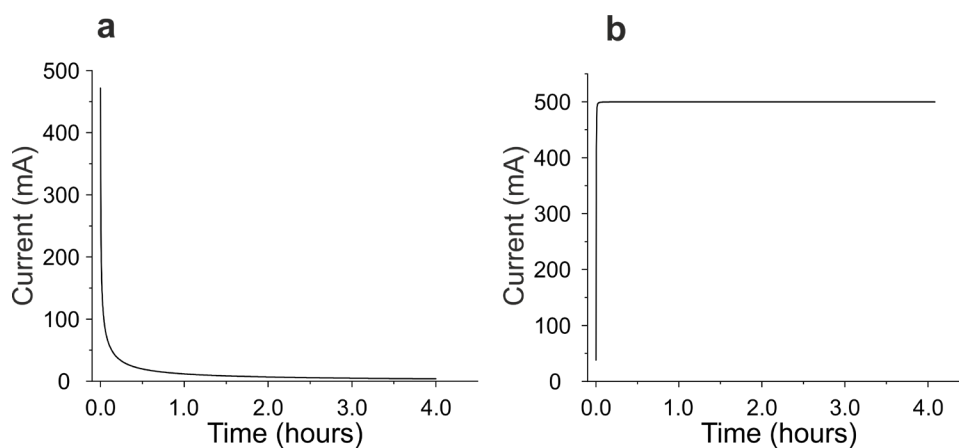


Fig. S2. The preparation of charged-sorbents. The activated carbon fabric ACC-5092-10 cloth was applied with a constant potential (a) 0.565 V vs SHE for the PCS-OH and (b) -0.235 V vs SHE for the NCS-K.

During the positive charging process, the integrated charge from chronoamperometry (CA) is larger than that calculated from the capacitance (**Table S1**). The charging current remained 12 mA after 4.8 hours. This implies that the positive charging process was accompanied by electrochemical carbon oxidation in the KOH electrolyte. However, the porous structure and pore size distribution of the sorbents only changed slightly (around 20% decrease in BET surface area). In contrast, the negative charging process gave the similar charge calculated from both the CA and capacitance measurements, and the charging current decayed to few hundreds nA after 40 min. This finding indicates that a chemical reaction (carbon oxidation) occurred during the positive charging process but not during the negative charging process.

Table S1. Comparison of charge passing for positively and negatively charging process.

	Integrated charge from CA (C)	Charge calculated from capacitance* (C)
Positive charging process	791.2	48
Negative charging process	38.6	48

* The charge is calculated based on the equation: $Q = C \times U$. Q is the charge passing in the charging process, C is the double layer capacitance (120 F g^{-1} for carbon fabric ACC-5092-10 cloth in the 6 M KOH at 0.4 V), U is the electric potential.

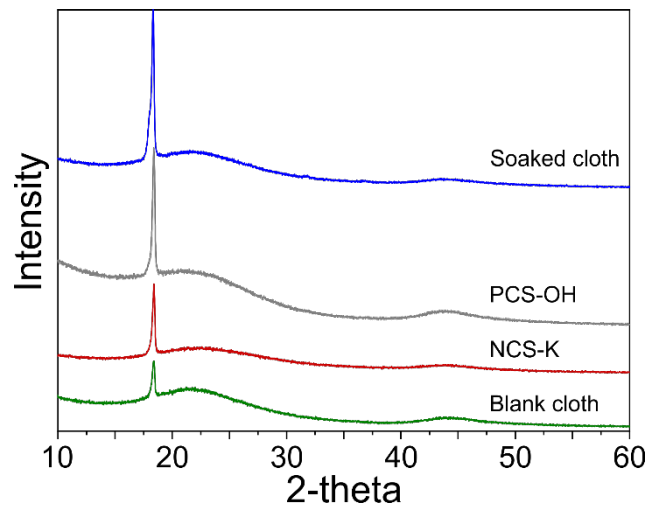


Fig. S3. Powder X-ray diffraction pattern (Cu K α radiation, $\lambda = 1.5406 \text{ \AA}$) of positively charged-sorbent, negatively charged-sorbent, soaked cloth and blank cloth. The peak at approximately 18° was present in all samples, and its origin is unknown.

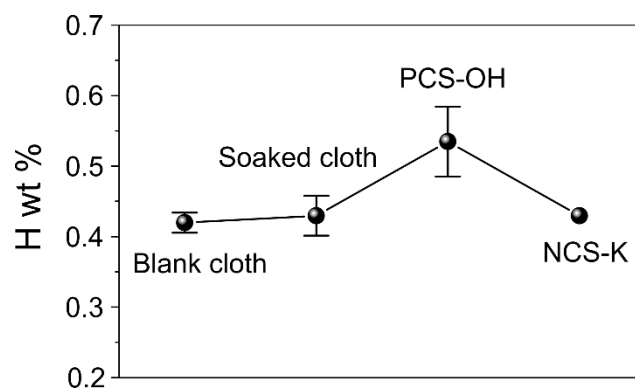


Fig. S4. The hydrogen weight percentage determined from combustion analysis from blank cloth, soaked cloth, PCS-OH and NCS-K. Standard deviations are calculated from 3 independent samples.

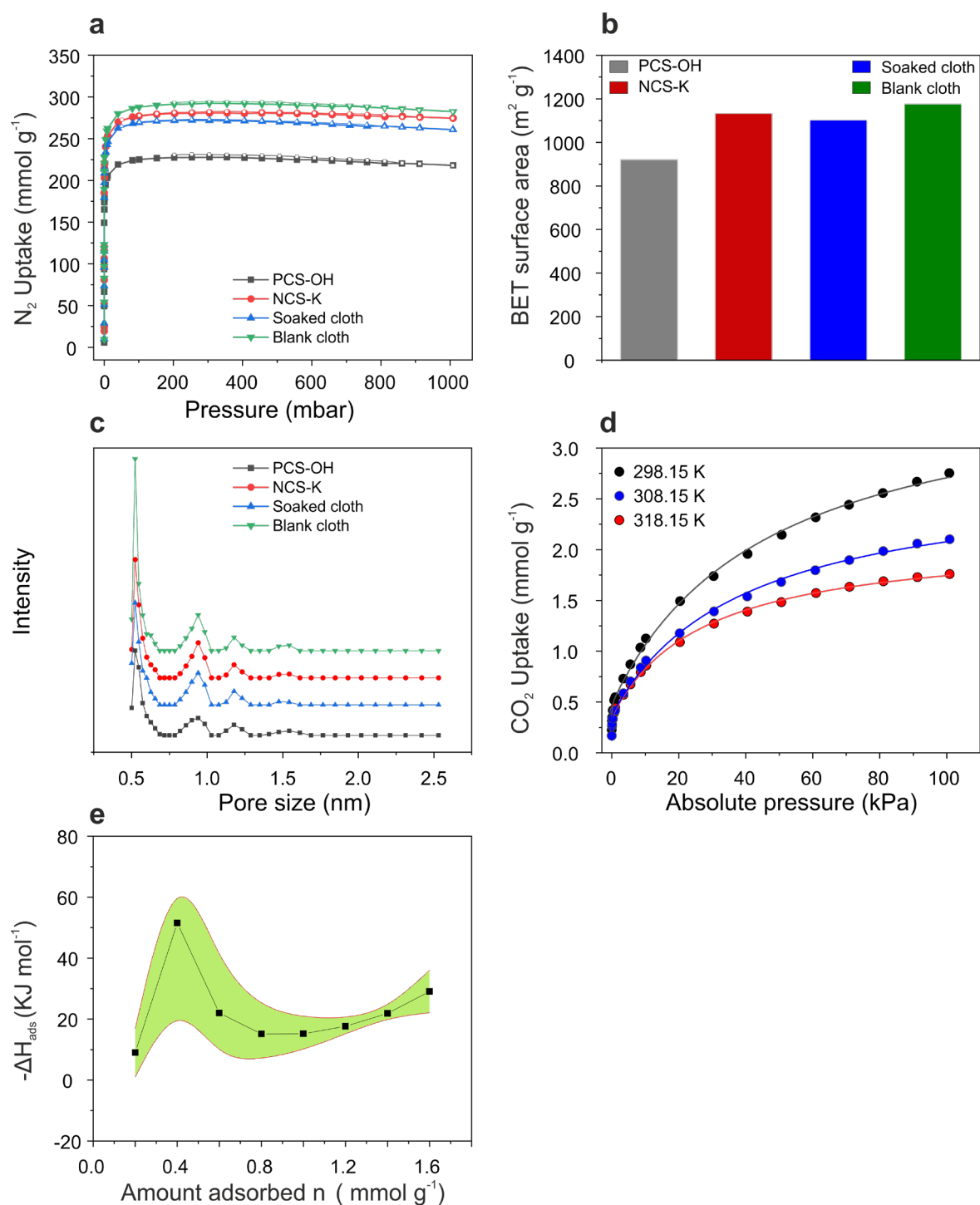


Fig. S5. (a) N_2 adsorption (filled circles) and desorption (open circles) isotherms of PCS-OH, NCS-K, soaked cloth, and blank cloth at 77 K. (b) BET surface areas derived from (a). (c) Pore size distributions derived from (a) using the nonlocal density functional theory (DFT). (d) CO_2 adsorption isotherms of activated PCS-OH at 298.15 K, 308.15 K, and 318.15 K. Solid lines represent fits to the dual-site Langmuir-Freundlich model. (e) Heats of adsorption ($-\Delta H_{ads}$) for CO_2 adsorption as a function of uptake for PCS-OH, as determined using the fits in (d). The standard deviations (green part) are calculated from the straight line fits of the data from three temperatures.

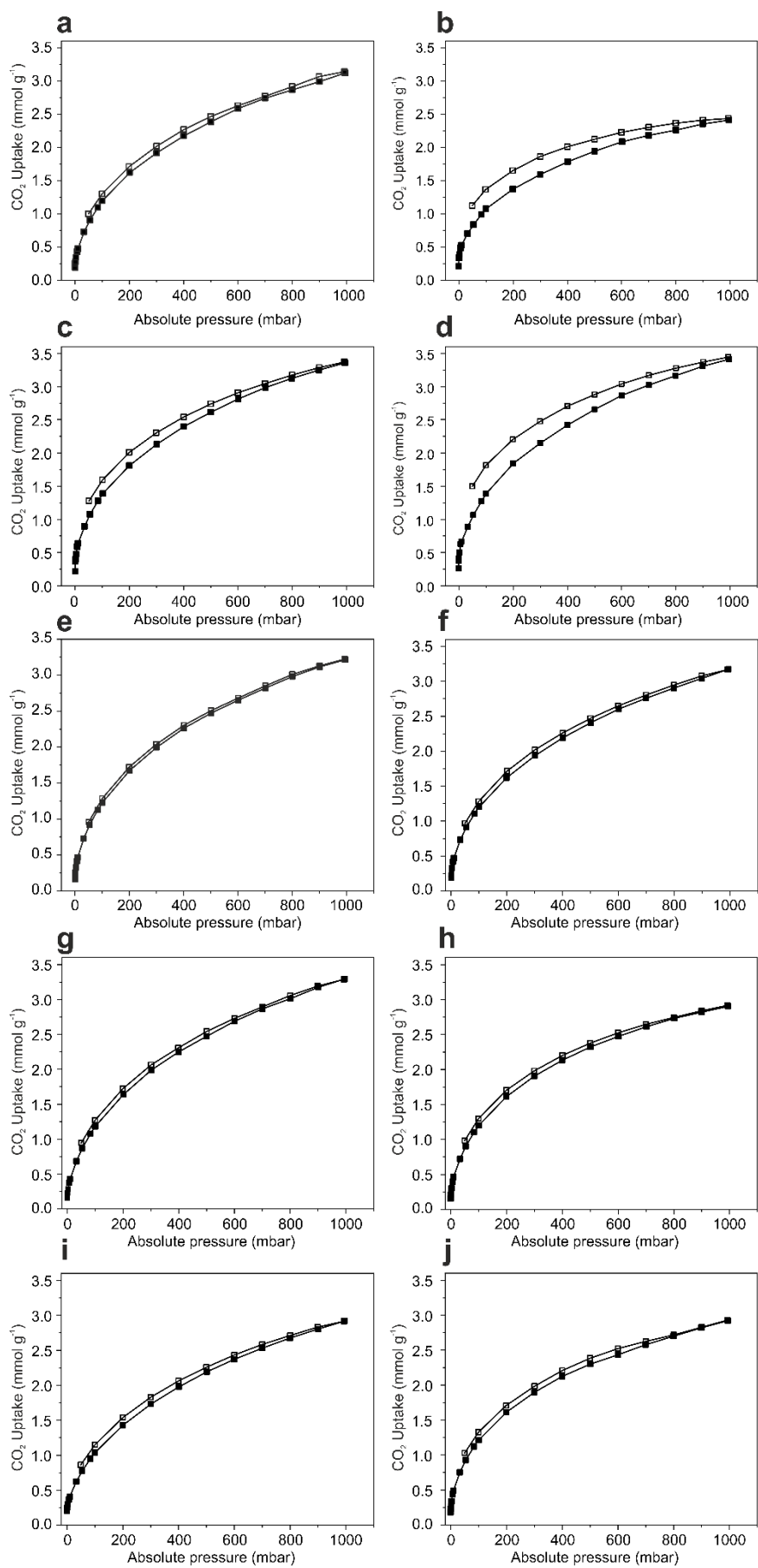


Fig S6 CO₂ sorption isotherms of 10 independent PCS-OH samples at 25 °C. The charging processes were conducted in the same conditions for all of the samples. Solid symbols for adsorption curves and hollow symbols for desorption ones.

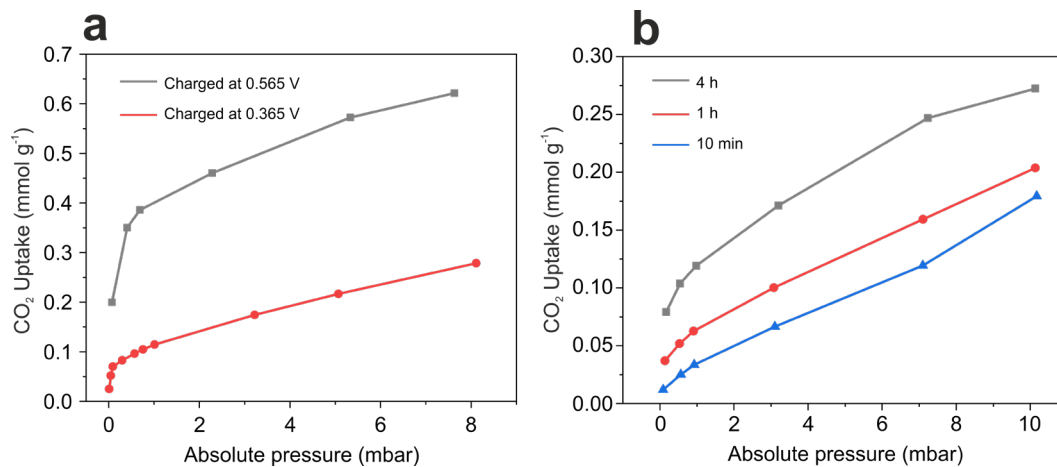


Fig S7 (a) CO₂ uptake of PCS-OH prepared at different potentials V for 4 h in three electrode configuration: 0.565 V and 0.365 V. **(b)** CO₂ uptake of PCS-OH prepared with various charging durations: 4 h, 1 h and 10 min. The charging processes were conducted in a Swagelok cell with potential holds at 0.565 V.

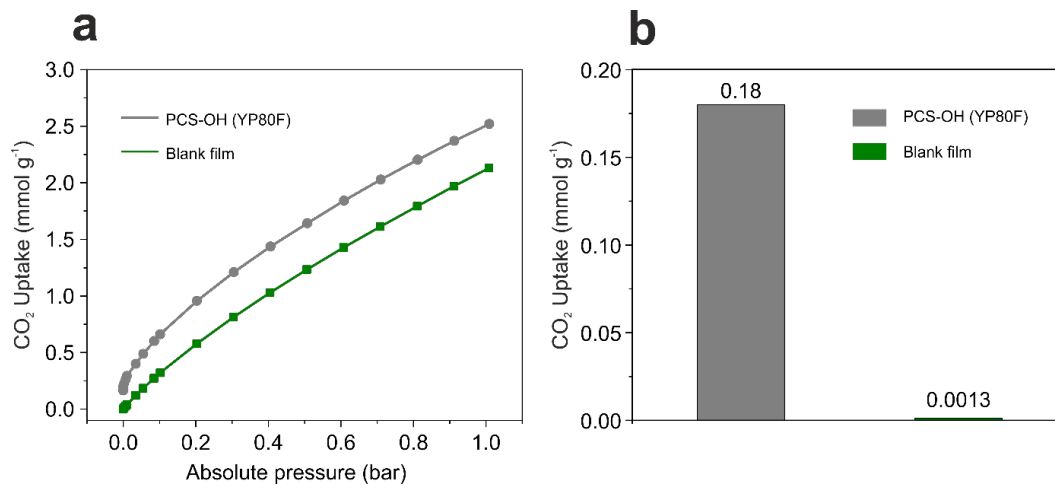


Fig S8 (a) CO₂ adsorption isotherms of PCS-OH made from YP80F activated carbon film, referred to as PCS-OH (YP80F), and control sample of YP80F activated carbon at 25 °C. **(b)** CO₂ uptake of PCS-OH (YP80F) and control sample of YP80F activated carbon at 0.4 mbar and 25 °C.

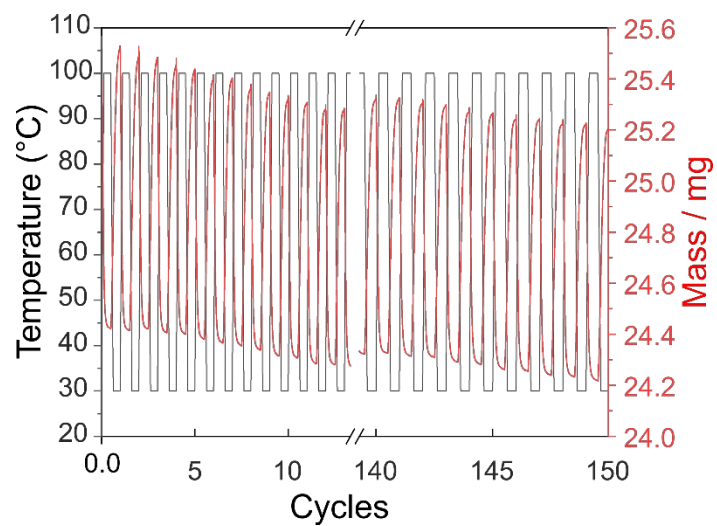


Fig. S9 Cycling capacities for 150 adsorption/desorption cycles for the PCS-OH in a simulated temperature-pressure swing adsorption process. Adsorption: 30 °C, 20 min, dry 30% CO₂ in N₂; Desorption: 100 °C, 20 min, dry 30% CO₂ in N₂.

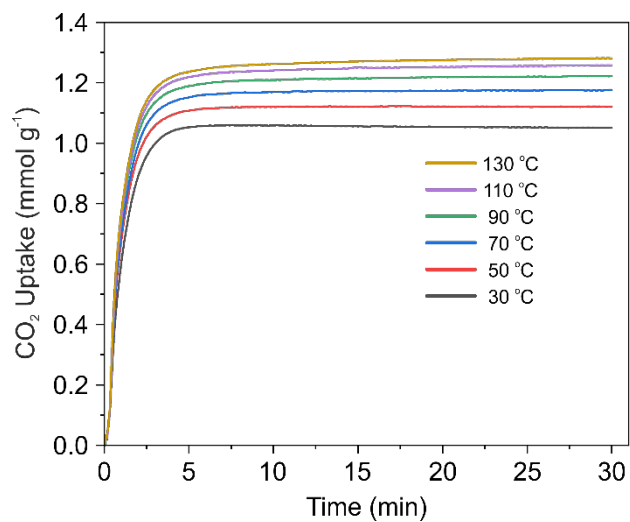


Fig. S10. CO₂ uptake curves at 40 °C and under 50% CO₂ in N₂ for PCS-OH after activation with various activation temperatures (130 °C, 110 °C, 90 °C, 70 °C, 50 °C and 30 °C).

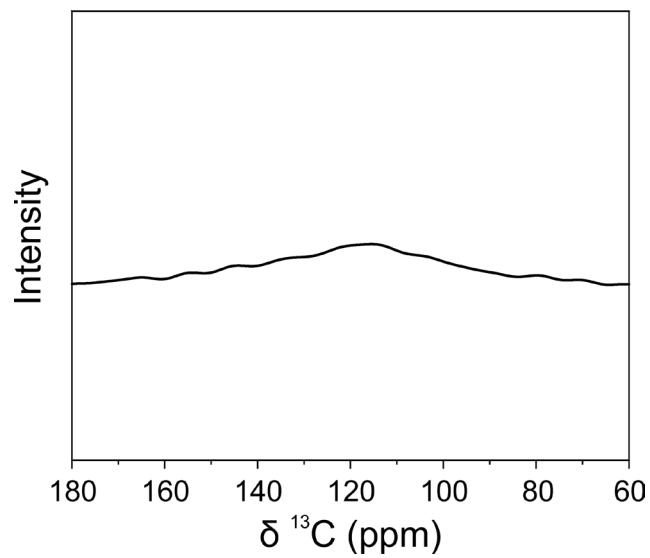


Fig. S11. ^{13}C ssNMR (9.4 T) spectrum of blank activated carbon cloth. A 90° pulse-acquire sequence was applied, and a sample MAS rate of 12.5 kHz was used. A broad resonance arising from sp^2 -hybridised carbon is observed.

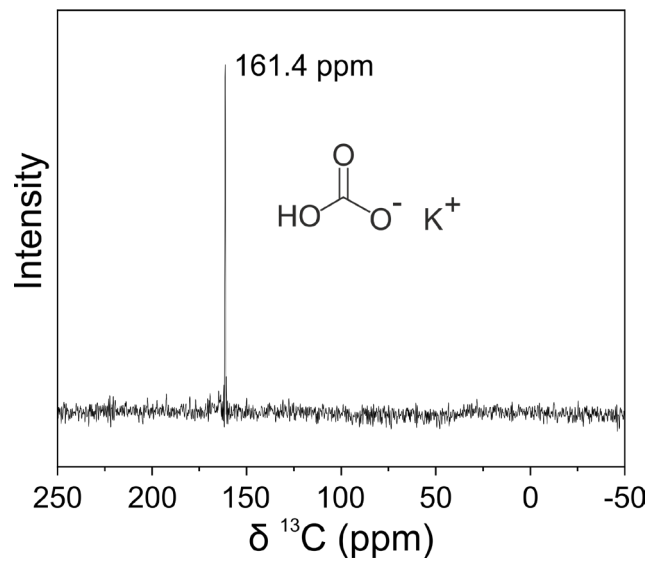


Fig. S12 ^{13}C ssNMR (9.4 T) spectrum of solid KHCO_3 . A 90° pulse-acquire sequence was used, with a sample MAS rate of 12.5 kHz.

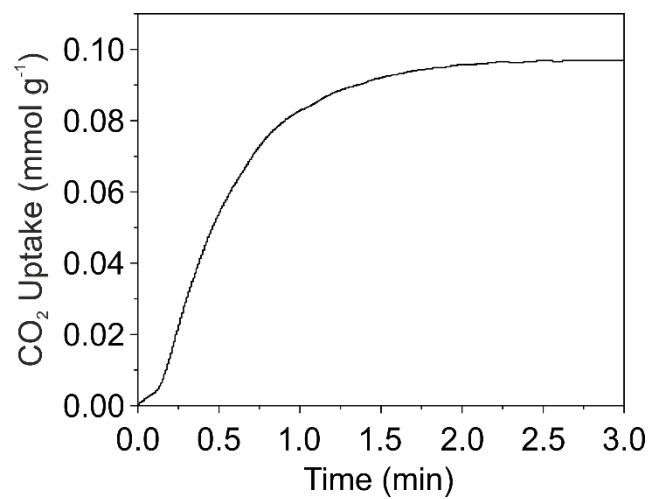


Fig. S13 CO₂ uptake curves at 40 °C and 400 ppm CO₂ in air for PCS-OH after activation under flowing dry N₂ at 130 °C for 1 h.

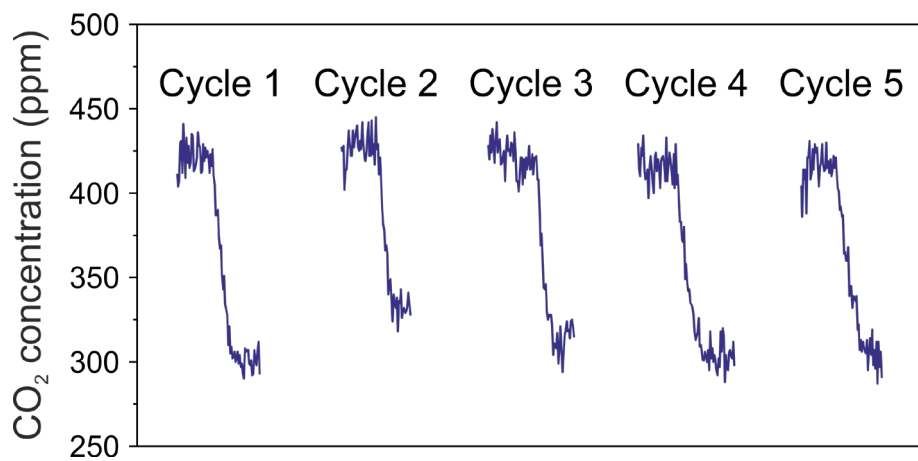


Fig. S14 Cycling capacities of DAC for the PCS-OH with Joule heating regeneration. The RH of DAC tests were controlled by desiccant (silica gel) at 11% at 25 °C. The mass of PCS-OH is 30 mg.

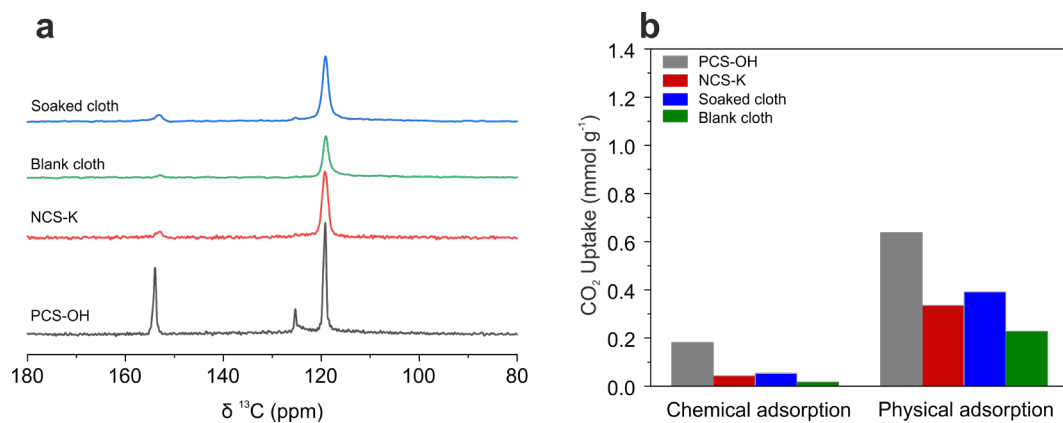


Fig. S15 (a) Quantitative ^{13}C solid-state NMR spectra of sorbents with $^{13}\text{CO}_2$ gas dosing at 0.9 bar, acquired at a MAS rate of 12.5 kHz. Prior to $^{13}\text{CO}_2$ dosing, the sorbents were pre-humidified using saturated salt solution (approximately 53% RH at 25 °C). **(b)** CO_2 uptake of sorbents via chemical and physical adsorption calculated from resonances at 156 ppm and 119 ppm of (a), respectively.

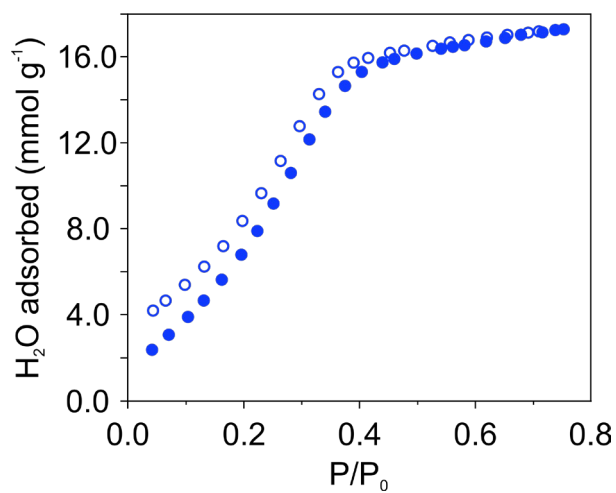


Fig. S16 H₂O adsorption (filled circles) and desorption (open circles) isotherms of the PCS-OH at 298.15 K.

Table S2. Comparison of kinetics of CO₂ uptake by selected adsorbents.

Samples	Kinetics for CO ₂ capture (mmol CO ₂ g ⁻¹ h ⁻¹)	Conditions	Reference
Composite PEI/Oxide	0.96 (30 °C)	400 ppm CO ₂	Ref. 1
Composite PEI/MMO	1.1 (25 °C)	400 ppm CO ₂	Ref. 2
PCS-OH	7.5 (40 °C)	400 ppm CO ₂	This work

References:

1. Sakwa-Novak, M. A., Tan, S. & Jones, C. W. Role of Additives in Composite PEI/Oxide CO₂ Adsorbents: Enhancement in the Amine Efficiency of Supported PEI by PEG in CO₂ Capture from Simulated Ambient Air. *ACS Appl. Mater. Interfaces* **7**, 24748–24759 (2015).
2. Zhu, X. *et al.* Efficient CO₂ Capture from Ambient Air with Amine-functionalized Mg–Al Mixed Metal Oxides. *J. Mater. Chem. A* **8**, 16421–16428 (2020).